International Journal of Steel Structures (2021) 21(1):118–131
https://doi.org/10.1007/s13296-020-00420-7

Online ISSN 2093-6311
Print ISSN 1598-2351

Dynamic Analysis of Semi-submersible Under the Postulated Failure of Restraining System with Buoy

Srinivasan Chandrasekaran[1] · **Syed Azeem Uddin**[1] · **Mubarak Wahab**[2]

Received: 26 March 2020 / Accepted: 21 September 2020 / Published online: 29 September 2020

Abstract
Coupled dynamic analyses of a deep-water Semi-submersible platform, in the South China Sea region, is carried out under postulated damage of the restraining system for both 10 and 100-years return period events. Under the combined action of wind, wave, and current loads, motion responses of Semi-submersible at 1500 and 2000 m water depths are analyzed in time-domain. Dynamic tension variations in the mooring lines are investigated for a fatigue failure using the S–N curve approach. Inclusion of a submerged buoy in the mooring system resulted in a marginal increase of the response due to a reduction in the restoration force of the mooring lines; submerged buoy also resulted in additional damping. The results of numerical studies showed an increase in tension in the mooring lines, which are adjacent to the damaged ones, causing reduced fatigue life. With the inclusion of submerged buoy in the mooring system, there is a considerable decrease in tension variation in mooring lines, increasing fatigue life. Failure of a mooring line causes an increase in tension of the adjacent mooring line, but not valid under all circumstances. It is seen from the studies that despite the postulated failure induced in a mooring, the adjoining line remains unaffected due to a steady coupling motion of the platform.

Keywords Coupled analysis · Fatigue analysis · Offshore platform · Postulated damage · Semi-submersible · Steel mooring

1 Introduction

Floating offshore platforms are designed and constructed to withstand harsh dynamic environmental loads. Semi-submersible is one of the floating offshore platforms, predominantly preferred over other alternatives because of its advantages, namely: better stability in harsh environments, larger deck area, superior constructional and installation features, and higher mobility. Preliminary studies showed that natural frequencies of Semi-submersible inversely vary with that of the draft and length of the platform. Therefore, the effects of change in length are dominant in comparison to their weight (Sunil and Mukhopadhyay 1995; Stansberg 2008). Researchers showed that the contribution of viscous forces in the splash zone is dominant, and affects the mean horizontal drift of the Semisubmersible (Dev and Pinkster 1995; Berthelsen et al. 2009). The Numerical studies carried out by Mavrakos et al. (1996) confirmed that there is a maximum reduction in the tension of mooring lines at the location of the buoy, contributing to maximum buoyancy.

Further, Mavrakos and Chatjigeorgiou (1997) reported that there is a decrease in the tension in mooring lines due to submerged buoys. Coupled dynamic analysis is essential to capture the effect of damping in the mooring lines that arise due to low-frequency motion (Ormberg and Larsen 1998; Clauss et al. 2002; Qiao and Ou 2013). The preliminary design of the GVA 4000 semi-submersible, as reported by Lee et al. (2005) confirmed that pontoon and column members are found to be safe even under harsh environmental loads. Chen et al. (2011) highlighted the influence of various parameters, namely tension-dip angle, pre-tension, configuration, and the number of mooring lines on the response of Semi-submersible.

Alternatively, hybrid mooring lines with a spread-mooring leads to loss of stability due to dynamic tension

✉ Srinivasan Chandrasekaran
drsekaran@iitm.ac.in

Syed Azeem Uddin
syedazeemuddina@gmail.com

Mubarak Wahab
mubarakwahab@utp.edu.my

[1] Department of Ocean Engineering, Indian Institute of Technology Madras, Chennai 600036, India

[2] Department of Civil and Environmental Engineering, Universiti Teknologi PETRONAS, Seri Iskandar, Malaysia

variations (Garza et al. 2000; Odijie et al. 2017). They showed that lesser inclination of mooring lines leads to the better dynamic behavior of the platform in the horizontal plane. It also results in more inferior strains and reduced stiffness of the mooring lines. Stability charts, along with the appropriate probabilistic tools, can be used to estimate the stability of the platform (Mao and Yang 2016). Hussain et al. (2009) showed that the presence of a second-tier pontoon reduces the heave motion of a deep-draft semi-submersible. Steel catenary risers (SCR) are recommended for semi-submersibles in the Gulf of Mexico (GoM) region to achieve a lesser offset. SCRs also showed increased damping under the combined action of waves and currents (Kim et al. 2011). Better motion characteristics of floating structures can be achieved by isolating the deck response (Chandrasekaran 2015, 2017a). However, a congested layout of topside modules shall also make the platform highly vulnerable to fire accidents (Chandrasekaran and Gaurav 2017). The design of the mooring system can influence the motion characteristics of semi-submersibles; however, damping offered by a spread-catenary mooring, with and without a buoy, does not change slow-drift motion (Hassan et al. 2009; Jang et al. 2019). In the case of compliant offshore platforms whose deck is partially isolated, deck response remains independent of the tension variations (Chandarsekaran and Vinothini 2019). Different sag-to-span ratios and the inclined angle of the mooring lines, under various current velocities also significantly affect the motion response of the floater and the tension in the mooring lines (Wang et al. 2018). On the other hand, deploying buoys in the mooring system reduces stress in the mooring lines and found to be effective in deep-water deployment (Xu et al. 2018).

Buoys, if provided at various sections along the mooring line, found to be further use as it increases fatigue life of steel mooring lines (Yan et al. 2018). (Xue et al. 2018) investigated a chain-fiber-chain mooring system for a Semi-submersible platform in the Gulf of Mexico region using the S–N curve, T–N curve, and fracture mechanics approach. For the safety factors recommended by the code, they showed that the results from the T–N curve and S–N curve are comparable while the former is marginally conservative. The fatigue life of the mooring chain is found to be sensitive towards the stress concentration factor for weld sections in mooring lines. Fatigue life anticipated by the fracture mechanics approach is ineffective with the depth of the crack. Gottlieb and Yim (1992) used the Liapunov function for analyzing the response under small excitations. The stability analysis for the response of lower-order systems is carried out by the harmonic balance method, leading to stability curves defining the loss of symmetry and period-doubling. The stability analysis of slack-mooring under the excitation of periodic waves using the harmonic balance method (HBM) is capable of handling system nonlinearity that arises from restoring forces of the mooring lines (Umar et al. 2004). A critical review, as reviewed above, showed the necessity of investigating Semi-submersible under a new mooring layout. A Semi-submersible, pegged with a new configuration of spread mooring system with a submerged buoy is numerically investigated in the present study. The motion of the platform induces dynamic tensions in the steel moorings, leading to fatigue damage. The fatigue life is estimated using the S–N curve approach for the postulated failure of the mooring lines.

2 Description of the Semi-submersible Model

A Semi-submersible platform chosen for the current study is shown in Fig. 1. It consists of two large rectangular horizontal pontoons, submerged to provide sufficient buoyancy. Four-column members equidistantly placed both in the longitudinal and transverse directions connecting the pontoon members and support the deck. Four horizontal braces attach the column members and provide lateral stability. The deck houses drilling activities, storage of accessories, living quarters, production housing, and a helipad. The description of Semisubmersible is shown in Table 1.

A sixteen-point, symmetric spread catenary mooring in the form of chain-wire-chain configuration is employed for position-restraining the Semisubmersible. The angle between mooring lines within a group is 5˚ while between each group is 75°, as shown in Fig. 2. Configuration and properties of the spread mooring system are shown in Tables 2 and 3. Steel moorings used in the present study possess a yield strength higher than 350 MPa (Chandrasekaran and Jain. 2016). A submerged buoy is attached at the end of middle-wire in the spread mooring system, whose details are given in Table 4.

The Semisubmersible is subjected to environmental loads that arise in the sea state prevailing in the South China Sea; wave heading angles considered for the study are (0, 45, 90°). API wind spectrum is used for delineating the effects of the wind, while the JONSWAP (Joint Offshore Sea Wave Project) spectrum is used for characterizing wave loads. The current force is considered as non-linearly varying for a water depth of 1500 m. The return periods of various events discussed in the analysis are summarized in Table 5 (Qiao and Ou 2013).

3 Numerical Analyses

The first step of the analysis is to obtain hydrodynamic coefficients, including damping and added mass, diffraction forces, Froude–Krylov forces, mean drift-forces,

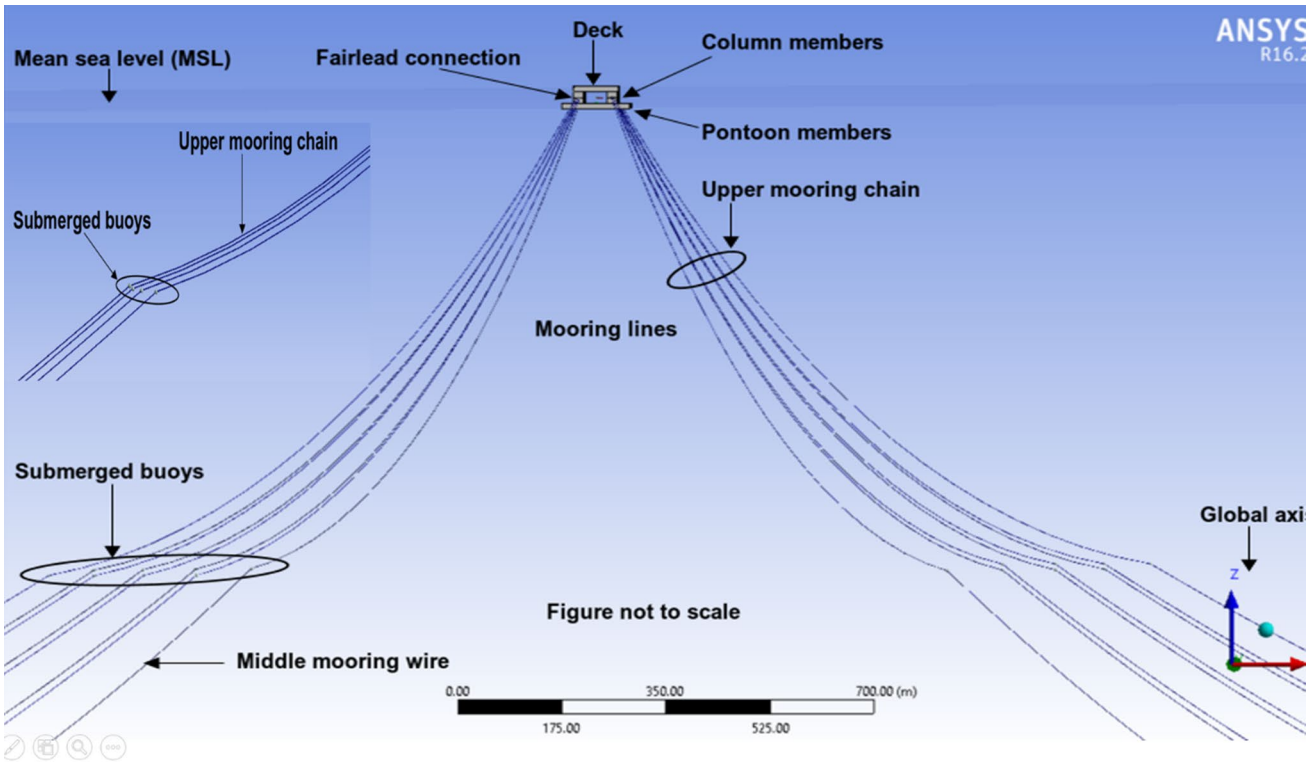

Fig. 1 Model of the semi-submersible

Table 1 Description of the semi-submersible

Description	Value	Units
Water depth	1500 m, 2000 m	m
Deck size	74.42 × 74.42 × 8.60	m
Displacement	48,206,800	kg
Pontoon members	114.07 × 20.12 × 8.54	m
Column members	17.385 × 17.385 × 21.46	m
Draft	− 19.00	m
Freeboard	19.60	m
Metacentric height	16.03	m
Centre of gravity	− 8.90	m
The radius of gyration (R_x)	32.40	m
The radius of gyration (R_y)	34.10	m
The radius of gyration (R_z)	34.40	m

response amplitude operators by diffraction analysis. The second step is to determine the motion response of the Semi-submersible coupled with mooring lines under the action of wind loads, current loads, first and second-order wave loads along with drag and inertia loads on the mooring lines. The hull of Semi-submersible is considered to be rigid, having six-degrees-of-freedom (d-o-f), while three d-o-f being translational, i.e., Surge, Sway and Heave and other three being rotational, i.e., Roll, Pitch and Yaw. Submerged section (wetted surface) of the Semi-submersible is discretized into many elements, and hydrodynamic coefficients are obtained by Greens function over the wetted surface.

In the present study, a time-domain analysis procedure is used and where step-wise time integration is performed for both the semi-submersible and mooring lines to account for the coupling action between them.

$$\begin{aligned}&\left[M + M_a\right]\ddot{x}(t) + [C]\dot{x} + [K]x \\ &\quad = F_{Environmental}(t) + F_{WF}(t) + F_{WDF}(t) + F_{Mooring}(t)\end{aligned} \tag{1}$$

where $[M]_{6\times6}$ is a mass matrix including an added mass matrix $\left[M_a\right]$, $[C]_{6\times6}$ indicates damping matrix, $[K]_{6\times6}$ is the stiffness matrix including hydrostatic stiffness, $\left\{F_{Enviromental}\right\}_{6\times1}$ is the external load vector including effects of wind, wave, and current, $\left\{F_{Mooring}\right\}_{6\times1}$ is the load vector due to spread catenary mooring, $\{x, \dot{x}$ and $\ddot{x}\}$ is the displacement, velocity, and acceleration vectors of Semisubmersible, F_{WF} is the wave frequency forces, F_{WDF} is the wave drift forces.

The effect of wave loading on the platform is evaluated using the diffraction theory with the boundary element method. JONSWAP spectrum is employed to include the impact of an irregular wave with slow drift on the platform. The spectral ordinate is given by:

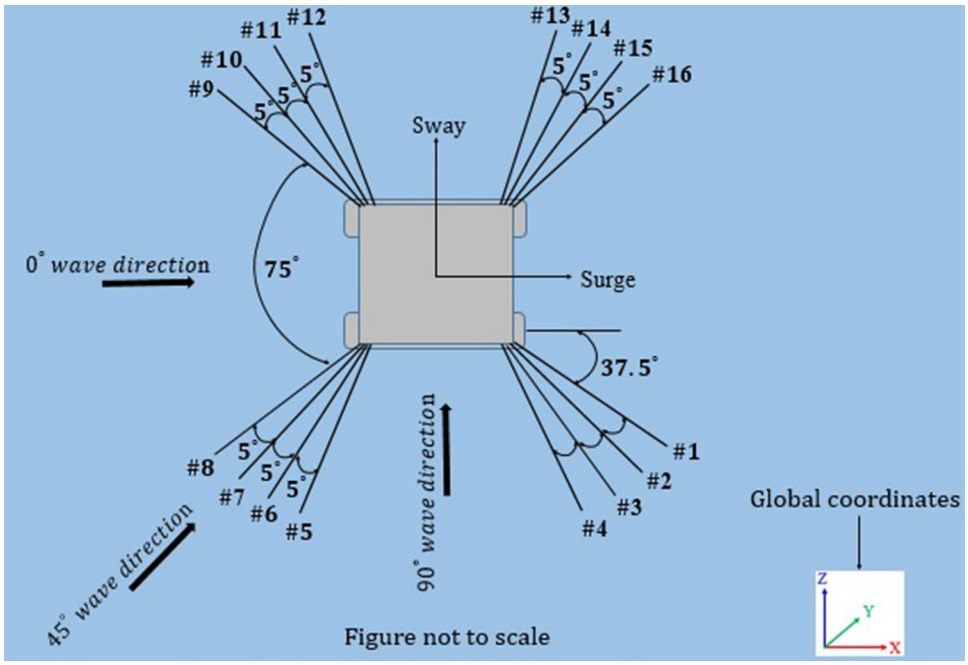

Fig. 2 Arrangement of the mooring (Plan view)

Table 2 Configuration of the mooring system

Water depth	Length of the spread catenary mooring		
	Upper chain	Middle wire	Lower chain
1500 m	300	2000	1500
2000 m	500	3000	1500

Table 3 Properties of the spread mooring system

Description	Upper chain	Middle wire	Lower chain
Mass per unit length (kg/m)	163.7	36.38	163.7
Stiffness, AE (N)	676,810,000	833,910,000	676,810,000
Equivalent diameter (m)	0.095	0.095	0.095
Longitudinal drag coefficient	1.15	0.025	1.15
Transverse drag coefficient	2.4	1.6	2.4
Added mass coefficient	1.0	1.0	1.0

Table 4 Description of the submerged buoy

Description	Value	Units
Diameter	5	m
Structural mass	5.861.6	kg
Displaced mass of water	6.7086	kg
Added mass	3.3543	kg
Coefficient of drag (C_d)	0.3	–
Coefficient of inertia (C_m)	0.5	–

Table 5 Environmental conditions of loads

Description	Return period		Units
	Ten years	100 years	
Significant wave height	11.1	13.3	m
Peak spectral period	13.6	15.5	sec
Peakedness parameter (Υ)	5	7	–
Wind speed	48.3	55	m/s
Current speed	1.7	1.97	m/s

'–' Indicates not applicable

$$S(\omega) = \frac{\alpha g^2 \gamma^a}{\omega^5} \times e^{\left(-\frac{5}{4}\times\left(\frac{\omega_p}{\omega}\right)^4\right)} \tag{2}$$

where ω = wave frequency (rad/s); ω_p = peak frequency (rad/s); g = acceleration due to gravity (m^2/s); Υ = Peakedness parameter or peak enhancement factor; a = spectral parameter (Eq. 3); α = spectral energy constant (Eq. 5); σ = spectral parameter (Eq. 4).

$$a = e^{\left(-\frac{(\omega-\omega_p)^2}{2\sigma^2\omega_p^2}\right)} \tag{3}$$

$$\sigma = \begin{cases} 0.09 & for\ \omega > \omega_p \\ 0.07 & for\ \omega \le \omega_p \end{cases} \tag{4}$$

$$\alpha = \frac{H_s^2}{16\int_0^\infty \frac{g^2\Upsilon^a}{\omega^5} \times \exp\left(\frac{-5}{4} \times \left(\frac{\omega_p}{\omega}\right)^4\right) d\omega} \tag{5}$$

API wind spectrum used to characterize the dynamic effects of wind loads is given by:

$$S(f) = \frac{\sigma(z)^2}{f} S\left(\breve{f}\right) \tag{6}$$

$$S\left(\tilde{f}\right) = \frac{\tilde{f}}{\left(1 + 1.5\tilde{f}\right)^{5/3}} \tag{7}$$

$$\tilde{f} = \frac{f}{f_p} and f_p = 0.025\left(\frac{V_Z}{Z}\right) \tag{8}$$

$$\overline{V}_z = \overline{V}_{10}\left(\frac{Z}{10}\right)^{0.125} \tag{9}$$

where $\tilde{f}$ is non-dimensional frequency; f and f_p are frequencies (Hz); $\overline{V}_z$ is the mean 1-h wind speed (m/s). The hydrodynamic loads acting on the Semi-submersible can be calculated by:

$$F_d = \frac{1}{2}\rho C_D D|u|u + \rho C_M A\dot{u} \tag{10}$$

$$F_d = \frac{1}{2}\rho C_D D|u|u - \frac{1}{2}\rho CD|\dot{x}|\dot{x} - \rho AC_M + \rho C_M A\dot{u} + \rho A\ddot{x}\left(1 + C_M\right) \tag{11}$$

Time-history responses of the semi-submersible, connected with mooring lines under the combined action of wind, wave, and current, are generated using the solver Ansys Aqwa. Second-order wave drift forces consisting of the slow-varying, low frequency (LF) effects, and mean drift forces are included in the analysis. Newman's approximation estimates the low-frequency forces. Wave-frequency (WF) forces consist of Froude–Krylov forces, diffraction wave forces, and radiation wave forces. The displacement and velocity of the motion of the platform are determined at each time-step, by integrating the acceleration in the time-domain, using the predictor–corrector integration scheme.

The natural periods and damping ratios for the Semi-submersible at 1500 m and 2000 m water depths, with and without a submerged buoy, are obtained from free-oscillation tests; results are shown in Table 6. It is seen from Table 6 that considerable periods in the surge, sway indicate higher flexibility about the horizontal plane. In contrast, small periods in roll, pitch, and heave show that they are stiff in the vertical plane. The natural periods in sway and yaw are found to be increased, along with a significant increase in the damping ratios for the surge, pitch, and yaw in the presence of a submerged buoy. It is interesting to note that a Semi-submersible platform is usually characterized by possessing free modes, indicating that the natural periods in all degrees-of-freedom are above the wave periods (DNV-RP-F205 2010).

4 Results and Discussion

4.1 Motion Responses Under the Postulated Failure of Mooring Lines

Coupled dynamic response of the platform in 1500 m water depth, obtained from the numerical analyses are plotted. Figures 3, 4, 5 shows the time-history of response in the surge, heave, and pitch under a ten year return period for (0°, 45°), respectively. It is seen from the figures that surge response is significantly higher in the case of postulated failure of mooring lines. Also, it could be observed that among all cases, mostly, the intact mooring without buoy has the lowest response.

Further, the presence of submerged buoy marginally increases the response for 0° wave heading. Surge response with intact mooring pegged with a submerged buoy is found

Table 6 Dynamic characteristics of moored semisubmersible

	Description	Surge	Sway	Heave	Roll	Pitch	Yaw
Without buoy							
1500 m water depth	T_n (s)	209	165	21	24	25	49
	ξ_n (%)	6.15	6.92	2.47	2.97	0.93	6.51
2000 m water depth	T_n (s)	193	184	25	25	25	54
	ξ_n (%)	5.84	6.38	4.15	4.75	1.91	7.98
With buoy							
1500 m water depth	T_n (s)	195	183	21	23	24	54
	ξ_n (%)	6.56	6.77	1.20	1.44	1.32	10.36
2000 m water depth	T_n (s)	213	199	21	23	24	53
	ξ_n (%)	6.87	6.21	1.45	1.06	0.83	4.61

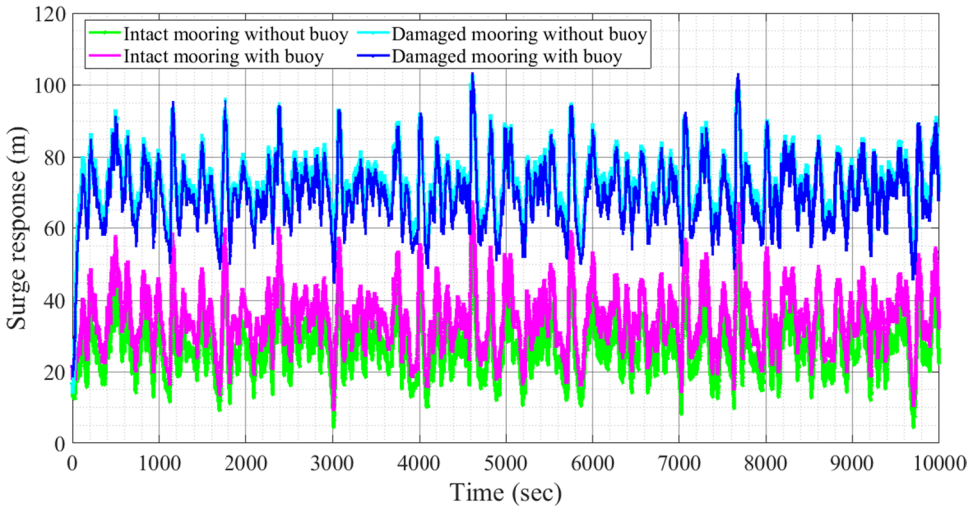

Fig. 3 Surge response under ten year return period (0°, 1500 m)

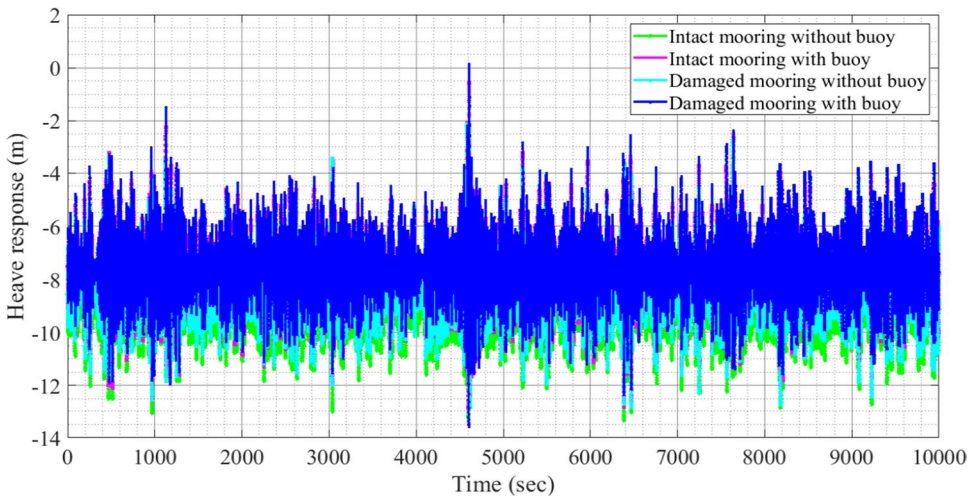

Fig. 4 Heave response under ten year return period (45°, 1500 m)

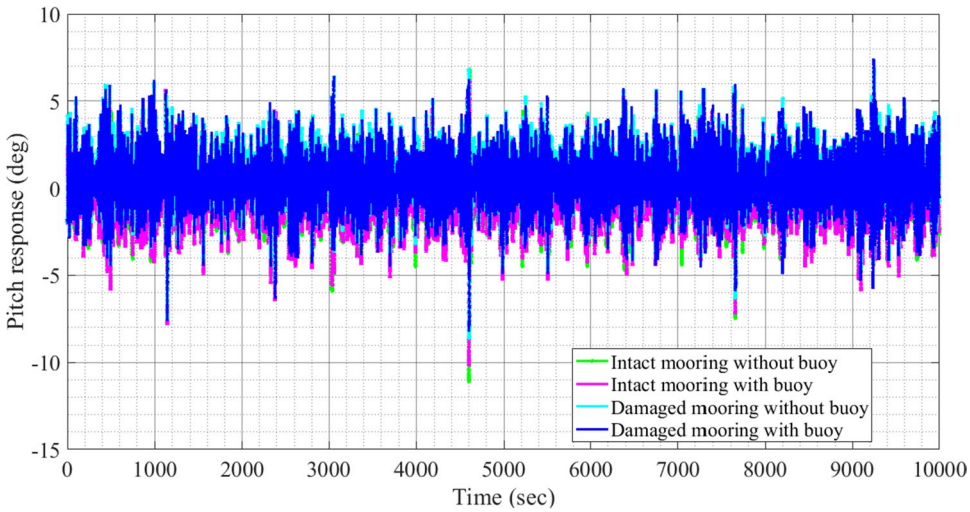

Fig. 5 Pitch response under ten years return period (0°, 1500 m)

to be higher, while during damage condition, surge response without buoy is significant. It can be due to additional damping of the buoy and higher added mass during the mooring failure condition.

The heave response showed in Fig. 4 has a quite similar variation among all the four cases. The standard deviation of heave responses is observed to be the highest among all the degrees-of-freedom during the failure condition, for the mooring lines pegged with a submerged buoy. Meanwhile, there is no significant difference in the heave response under both the intact and postulated failure conditions in the absence of a buoy; it is attributed to the symmetry of the incident wave to the chosen mooring configuration. The maximum pitch response is about 7° under the postulated failure condition (Fig. 5), which shows a marginal increase in the presence of buoy. However, this response is well below the permitted limits recommended by the code DNV-OS-E301 (2008).

4.2 Coupled Responses Under the Postulated Failure of the Mooring Lines

The power spectral density plots are obtained for the coupled response of the platform under the postulated failure condition. Figures 6, 7, 8 show the power spectral density plots of the surge, heave, and pitch responses, respectively. It is seen from the figures that natural frequencies of heave and pitch are tightly coupled but well placed away from that of the wave frequency. The other peaks, seen in the closer proximity to that of the surge (Fig. 6), are deduced from the irregular waves with slow-drift response. For 45° wave direction, as seen in Fig. 7, smaller peaks appearing near the wave frequency are due to the second-order effects of combined wind, wave, and current loading; as such, this effect is more for 0° pitch response, as seen in Fig. 8.

4.3 Tension Variation in Mooring Lines Under Postulated Failure

The platform is investigated under the postulated failure condition of the selected set of mooring under different wave heading angles. All mooring lines are pegged with a buoy to envisage reduced response (Mavrakos and Chatjigeorgiou 1997). Figures 9, 10, 11 show the tension variation time history of a different set of mooring under the ten year return period and 1500 m water depth; Figs. 12,13,14 shows the variation for 2000 m water depth. It can be seen from Fig. 9 that the tension variation in the mooring line #11 under the postulated failure of (#10, #12) is found to be increased by about three times its original tension. It arises from the additional loads transferred from the failed moorings (Chandrasekaran and Uddin 2020). As seen in Fig. 10, for a 45° wave heading, mooring lines #9 and #10 are failed conditions under ten years return period. It causes an increase in the tension of the mooring lines (#11, #12), which are adjacent to the damaged mooring lines (#9, #10), as seen in Figs. 9 and 13.

As seen in Fig. 11, for a 90° wave heading under ten years return period, the tension in mooring lines #1 & #15 is observed to have marginally increased due to load transfer

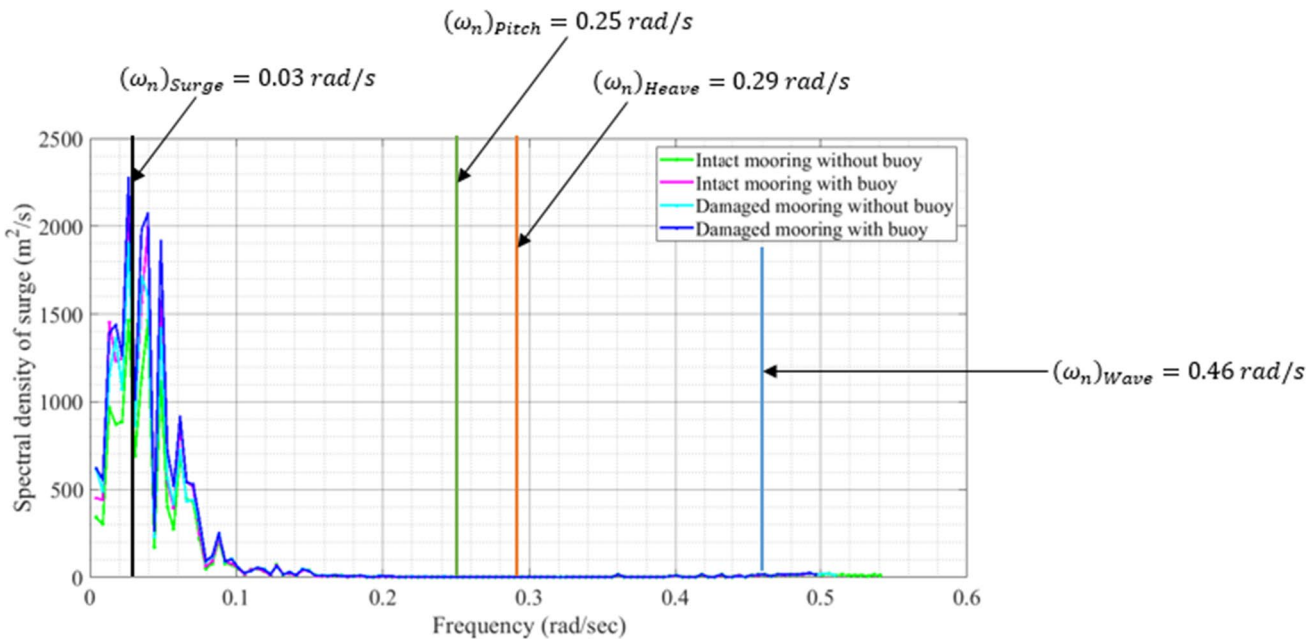

Fig. 6 Power spectral density for the surge for a ten year return period (0°, 1500 m)

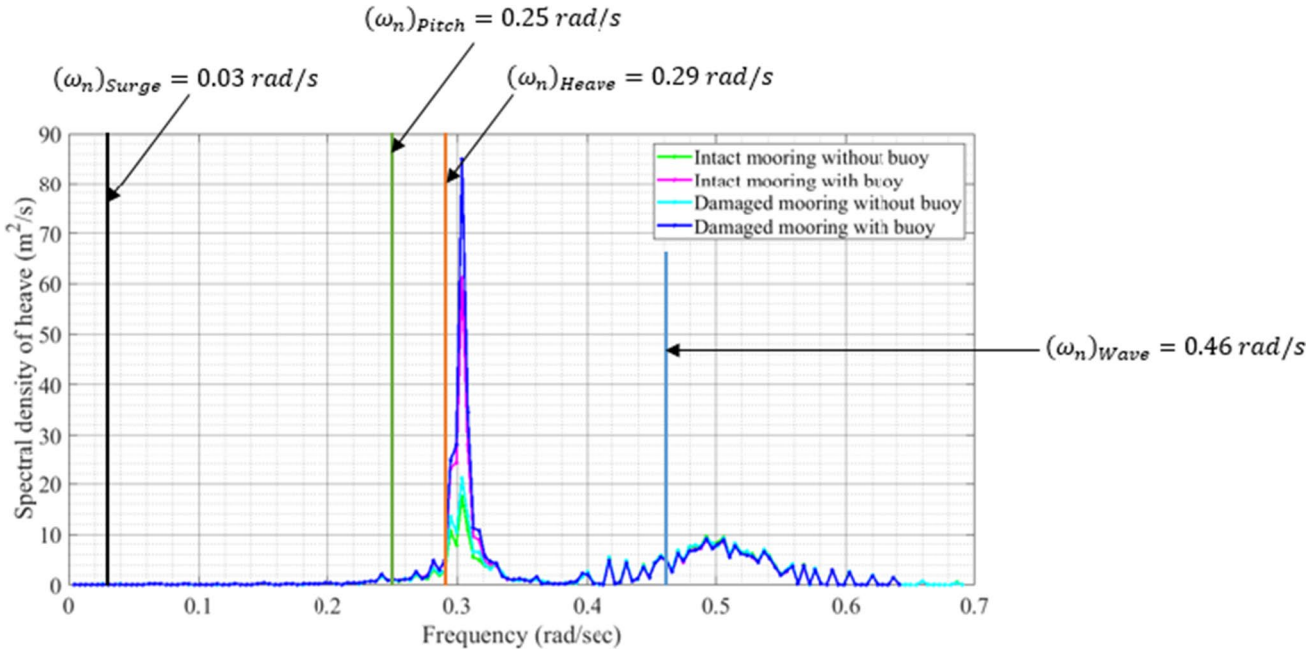

Fig. 7 Power spectral density for the heave for a ten year return period (45°, 1500 m)

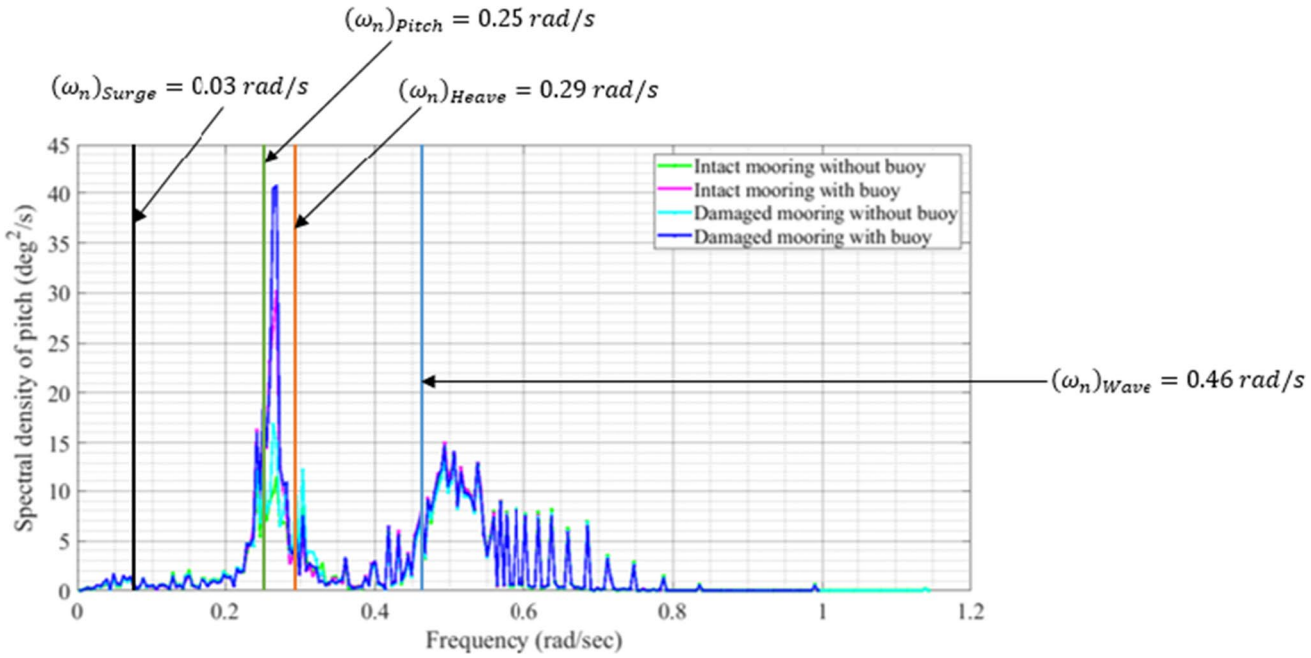

Fig. 8 Power spectral density for the pitch for a ten year return period (0°, 1500 m)

from the failed mooring lines #2 and #14. Figure 12 shows that the tension variation in the mooring line #2, under the influence of damaged mooring line #1, is found to be significant in comparison to that of mooring line #13; it is due to the effect of coupled responses. Due to the effect of coupling responses at 45° direction of wave loading, the tension in the mooring lines #12 & #15 is slightly increased (Fig. 13). Under increased water depth of 2000 m, as seen in Fig. 14, the tension in mooring lines #1 and # 14 has rapidly increased, due to the failure of the adjacent mooring lines #15 and #16. But, this increase is not significant due to the un-symmetric transfer of failure mooring loads to the adjacent mooring lines and direction of environmental loadings (Chandrasekaran and Uddin 2020).

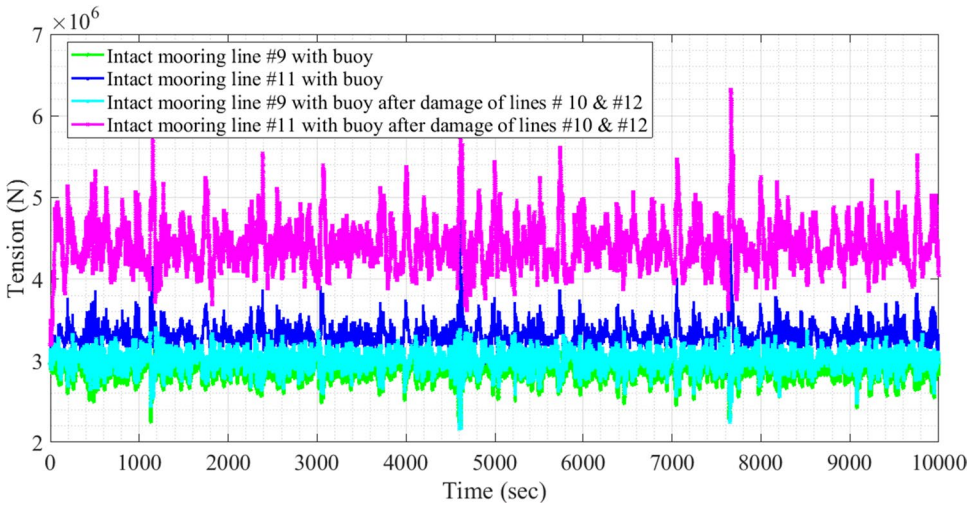

Fig. 9 Tension variation in mooring (9, 11) for ten years return period (0°, 1500 m)

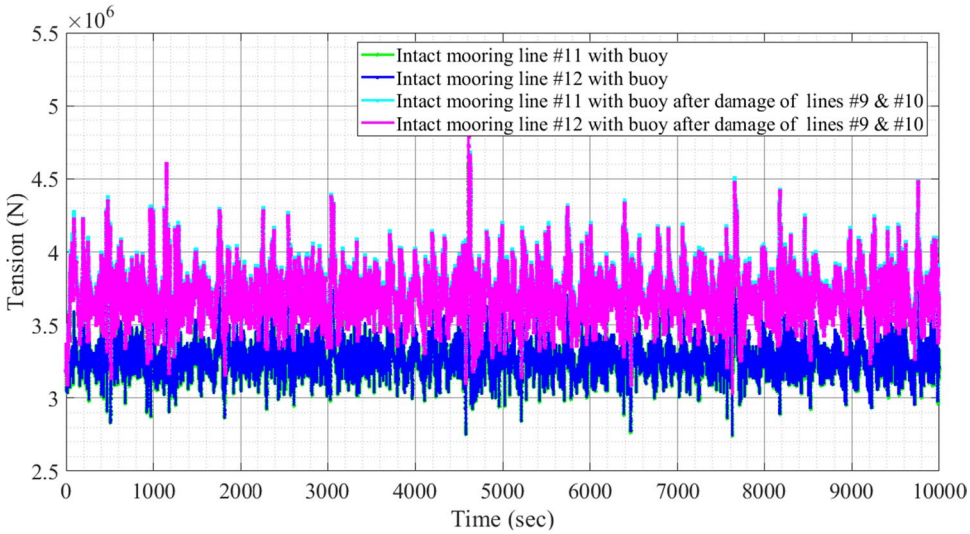

Fig. 10 Tension variation in mooring (11, 12) for ten years return period (45°, 1500 m)

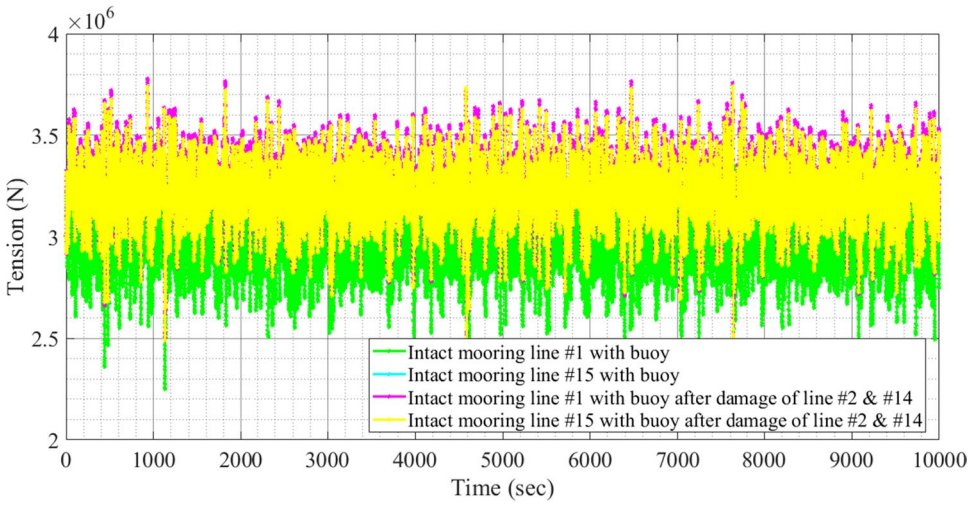

Fig. 11 Tension variation in mooring (1, 15) for ten years return period (90°, 1500 m)

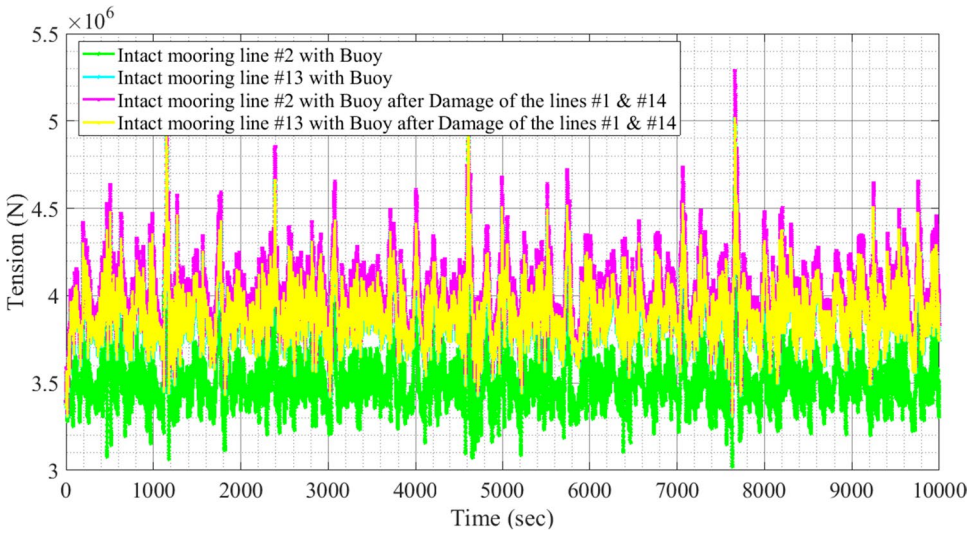

Fig. 12 Tension variation in mooring (2, 13) for ten years return period (0°, 2000 m)

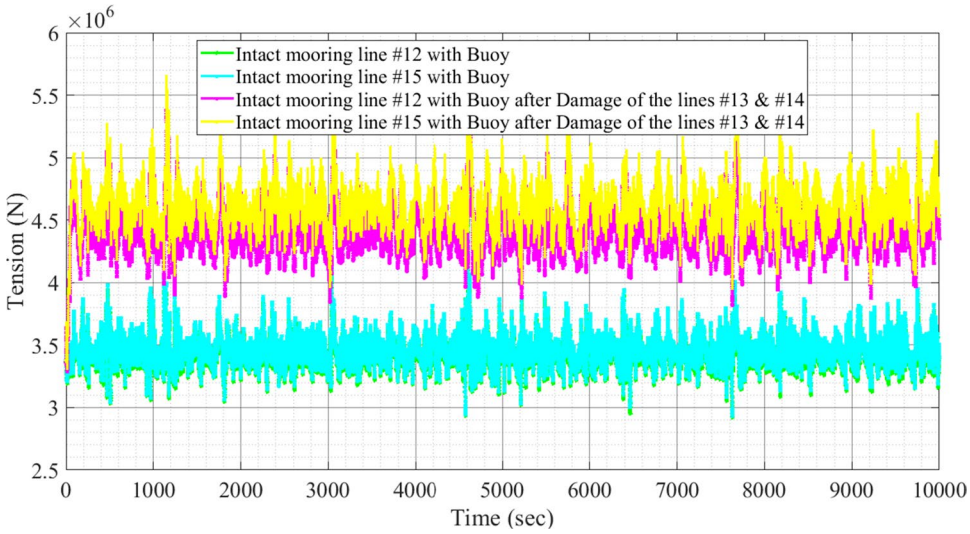

Fig. 13 Tension variation in mooring (12, 15) for ten years return period (45°, 2000 m)

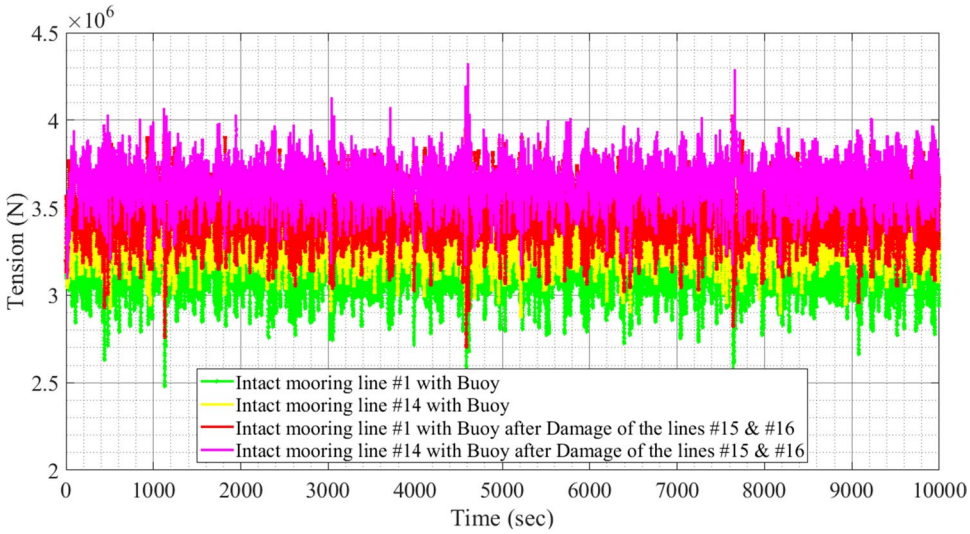

Fig. 14 Tension variation in mooring (1, 14) for ten years return period (90°, 2000 m) water depth

5 Fatigue Analysis

The fatigue life of mooring lines, both under intact and postulated failure conditions are estimated using Palmgren–Miners rule. The dynamic tension variation in the moorings, under the motion of Semi-submersible, induces a large number of stress cycles, resulting in fatigue damage. The S–N curve approach is used to estimate the number of cycles required to cause fatigue damage. The pre-tension of the mooring causes stress response of the mooring lines to be a non-zero mean process. After deducing the stress ranges and averages of the cycles, each cycle is subsequently converted into an equivalent stress range of a zero-mean process using the Goodman diagram. According to the Palmgren-Miners rule, fatigue failure of the mooring line will occur when the strain energy of variable amplitude (n) is equal to that of the constant amplitude cycle (N); it is given as below:

$$D = \sum_{i=1}^{m} \frac{n_i}{N_i} \tag{12}$$

where 'n_i' is the number of cycles per year for a given tension range interval, and 'N_i' is the cycles to failure under tension range 'i' according to the S–N curve. The parameters for the S–N curve are chosen according to the standards (DNV-RP-C203 2005), and fatigue life is then calculated from the estimated damage and then extrapolated for 10,000 s to obtain fatigue life of the mooring lines. Figures 15, 16, 17 show the fatigue life expected for mooring lines, both under intact and failed condition, respectively under 1500 and 2000 m water depths; both are estimated in the presence of buoy. It is seen from the figures that the

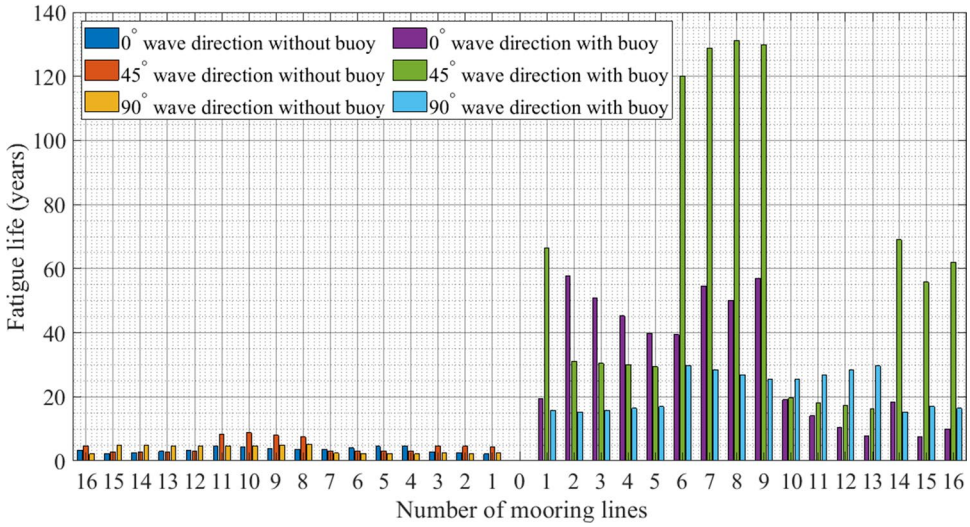

Fig. 15 The fatigue life of the mooring lines (10 years return period, 1500 m) under intact conditions

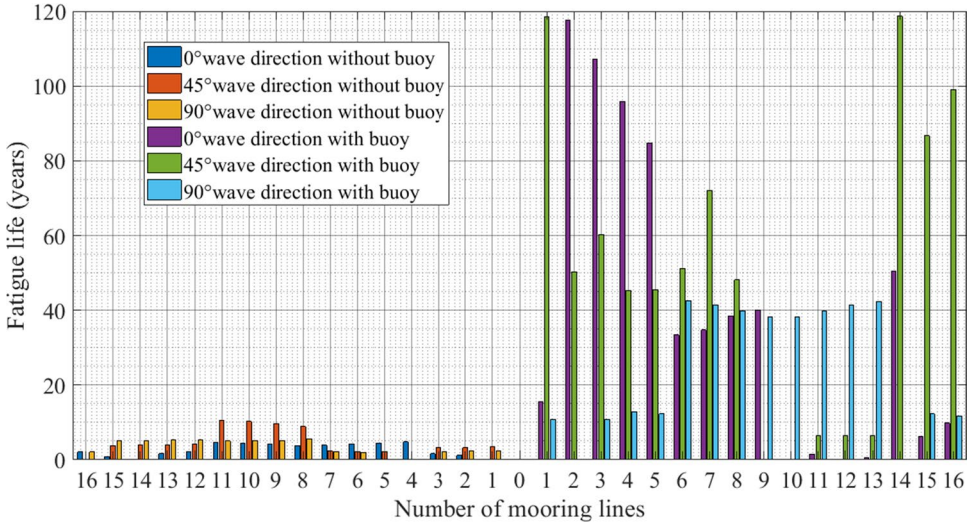

Fig. 16 The fatigue life of the mooring lines (10 years return period, 1500 m) under postulated failure conditions

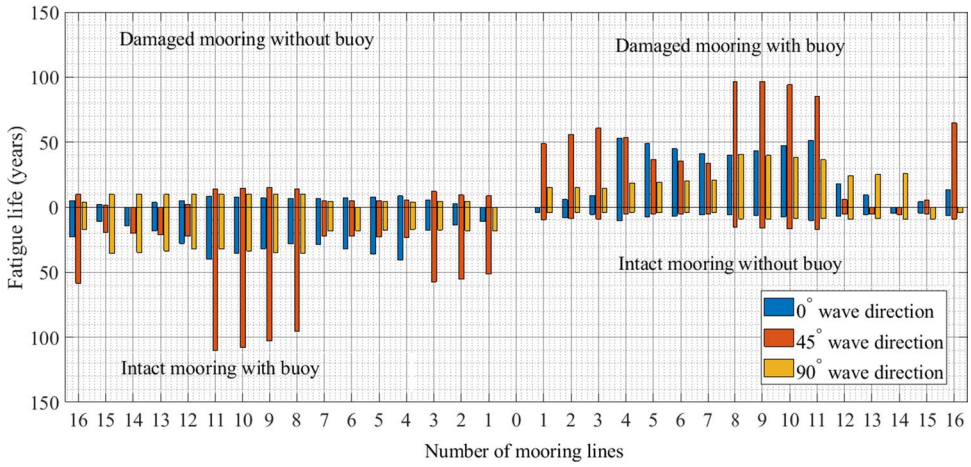

Fig. 17 The fatigue life of mooring lines (10 years return period, 2000 m)

inclusion of submerged buoys increased fatigue life significantly (Mavrakos and Chatjigeorgiou 1997; Chandrasekaran and Uddin 2020). It is also important to note that the fatigue life of intact lines without buoy showed lesser fatigue life in comparison to those with a submerged buoy.

6 Conclusions

Coupled dynamic analysis of a semi-submersible with symmetric spread mooring is carried out under a postulated failure condition for different wave heading angles. The mean responses of the platform are found to marginally increase with the inclusion of buoy in the mooring system. It is due to the decrease in the restoration force, but the responses are within the permissible limits. Dynamic tension variations caused in the mooring under the postulated failure condition resulted in fatigue failure. With the inclusion of the submerged buoy in the mooring system, there is a considerable decrease in tension variation in the mooring lines, increasing fatigue life. Failure of a mooring line causes an increase in tension of the adjacent mooring line, but not valid under all circumstances. It is seen from the studies that despite the postulated failure induced in a mooring, the adjacent line remains unaffected due to a strong coupling motion of the platform.

Appendix

See Table7

Table 7 Statistics of Semi-submersible under postulated failure conditions for various positions of the buoy in the mooring system

D-o-f	Statistics	Case-1			Case-2			Case-3			Case-4		
		0°	45°	90°	0°	45°	90°	0°	45°	90°	0°	45°	90°
Surge	Min	49.39	3.1	−39.18	18.73	5.37	−0.02	16.51	8.92	−0.01	12.2	−28.7	−39.92
	Max	102.7	27.42	−0.01	103.22	32.12	−0.006	78.66	40.66	39.79	76.97	12.34	−0.01
	Mean	72.41	14.07	−36.35	69.53	17.16	−0.01	43.77	24.68	34.17	40.5	−15.42	−32.54
	S.D	8.11	3.36	1.98	9.43	3.68	0.003	9.6	3.93	1.87	9.97	4.21	1.87
Heave	Min	−15.42	−12.83	−12.13	−14.96	-13.6	−11.82	−14.25	−13.74	−11.8	−14.08	−12.78	−11.76
	Max	−0.3	−2.1	−3	0.98	0.13	−2.02	1.45	0.19	−1.98	1.76	0.46	−1.64
	Mean	−8.4	−8.37	−8.4	−7.58	−7.55	−7.57	−7.56	−7.55	−7.58	−7.44	−7.42	−7.45
	S.D	1.21	1.18	1.05	1.38	1.39	1.11	1.36	1.44	1.12	1.43	1.46	1.16
Pitch	Min	−8.64	−6.81	−2.32	−8.15	−5.25	−0.005	−9.67	−5.29	−0.12	−9.63	−6.37	−1.91
	Max	6.9	5.06	0.08	7.41	4.58	0.004	6.11	4.67	2.0	6.2	3.48	0.13
	Mean	0.61	−0.1	−0.84	0.36	−0.12	−7.30E–05	−0.26	−0.07	0.69	−0.29	−0.78	−6.70E–01
	S.D	1.55	1.07	0.08	1.67	1.14	0.001	1.66	1.16	0.07	1.7	1.21	0.09

S.D indicates the standard deviation

Case 1, Mooring lines without the buoy; *Case 2*, Mooring lines with buoys at the end of the upper chain section; *Case 3*, Mooring lines with buoys at the end of the middle wire section; *Case 4*, Mooring lines with buoys at the end of the upper chain and middle wire sections

References

Berthelsen, P. A., Baarholm, R., Stansberg, C. T., Hassan, A., Downie, M., & Incecik, A. (2009). Viscous drift forces and responses on a semi-submersible platform in high waves. In *ASME 2009 28th International Conference on Ocean, Offshore and Arctic Engineering* (pp. 469–478). American Society of Mechanical Engineers Digital Collection.

Chandrasekaran, S. (2015). *Dynamic analysis and design of ocean structures*. Springer, India. ISBN: 978-81-322-2276-7.

Chandrasekaran, S., & Jain, A. K. (2016). *Ocean structures, Construction, Materials, and Operations. CRC Press, Florida.*ISBN: 978-149-87-9742-9

Chandrasekaran, S. (2017, a). *Dynamic analysis and design of ocean structures*. Springer, 2nd Edition, Singapore. ISBN: 978-81-322-2276-7.

Chandrasekaran, S., & Gaurav S (2017). *Design aids for offshore structures under special environmental loads, including fire resistance.* Springer, Singapore. ISBN: 978-981-322-10-7608-7

Chandrasekaran, S., & Nagavinothini, R. (2019). Offshore triceratops under impact forces in ultra-deep arctic waters. *International Journal of Steel Structures*. https://doi.org/10.1007/s13296-019-00297-1.

Chandrasekaran, S., & Uddin, S. A. (2020). Postulated failure analyses of a spread-moored semi-submersible. *Innovative Infrastructures Solutions, 5*(2), 1–16. https://doi.org/10.1007/s41062-020-0284-2.

Chen, P., Chai, S., Ma, J., (2011). Performance evaluations of taut-wire mooring systems for the deep-water Semi-submersible platform. In *ASME 2011 30th International Conference on Ocean, Offshore and Arctic Engineering*, 207–2015, https://doi.org/10.1115/OMAE2011-49281

Clauss, G., Schmittner, C., & Stutz, K. (2002). Time-domain investigation of a semi-submersible in rogue waves. In *ASME 2002 21st International Conference on Offshore Mechanics and Arctic Engineering* (pp. 509–516). American Society of Mechanical Engineers Digital Collection, https://doi.org/10.1115/OMAE2002-28450

Dev, A. K., & Pinkster, J. A. (1995). Viscous mean drift forces on moored Semi-submersibles. In *The Fifth International Offshore and Polar Engineering Conference*. International Society of Offshore and Polar Engineers.

DNV-OS-E301, 2008. Position mooring, 33–34.

DNV-RP-C203, 2005. Fatigue design of offshore steel structures, 14–16.

DNV-RP-F205, 2010. Global Performance Analysis of Deepwater Floating Structures.

Garza-Rios, L. O., Bernitsas, M. M., Nishimoto, K., & Matsuura, J. O. P. J. (2000). Dynamics of spread mooring systems with hybrid mooring lines. *Journal of Offshore Mechanics and Arctic Engineering, 122*(4), 274–281. https://doi.org/10.1115/1.1315591.

Gottlieb, O., & Yim, S. C. (1992). Nonlinear oscillations, bifurcations, and chaos in a multi-point mooring system with a geometric nonlinearity. *Applied Ocean Research, 14*(4), 241–257. https://doi.org/10.1016/0141-1187(92)90029-J.

Hassan, A., Downie, M. J., Incecik, A., Baarholm, R., Berthelsen, P. A., Pakozdi, C., & Stansberg, C. T. (2009). Contribution of the mooring system to the low-frequency motions of a semi-submersible in combined wave and current. In *ASME 2009 28th International Conference on Ocean, Offshore and Arctic Engineering* (pp. 55–62). American Society of Mechanical Engineers Digital Collection, https://doi.org/10.1115/OMAE2009-79074

Hussain, A., Nah, E., Fu, R., & Gupta, A. (2009). Motion comparison between a conventional deep draft Semi-submersible and a dry tree Semi-submersible. In *ASME 2009 28th International Conference on Ocean, Offshore and Arctic Engineering* (pp. 785–792). American Society of Mechanical Engineers Digital Collection, https://doi.org/10.1115/OMAE2009-80006

Jang, B. S., Kim, J. D., Park, T. Y., & Jeon, S. B. (2019). FEA based optimization of Semi-submersible floater considering buckling and yield strength. *International Journal of Naval Architecture and Ocean Engineering, 11*(1), 82–96. https://doi.org/10.1016/j.ijnaoe.2018.02.010.

Kim, Y., Kim, K. H., Kim, J. H., Kim, T., Seo, M. G., & Kim, Y. (2011). Time-domain analysis of nonlinear motion responses and structural loads on ships and offshore structures: development of WISH programs. *International Journal of Naval Architecture and Ocean Engineering, 3*(1), 37–52. https://doi.org/10.2478/IJNAOE-2013-0044.

Lee, Y., Incecik, A., & Chan, H. S. (2005). Prediction of Global Loads and Structural Response Analysis on A Multi-Purpose Semi-submersible. In *ASME 2005 24th International Conference on Offshore Mechanics and Arctic Engineering* (pp. 3–13). American Society of Mechanical Engineers Digital Collection, https://doi.org/10.1115/OMAE2005-67003

Mao, H., & Yang, H. (2016). Parametric pitch instability investigation of Deep Draft Semi-submersible platform in irregular waves. *International Journal of Naval Architecture and Ocean Engineering, 8*(1), 13–21. https://doi.org/10.1016/j.ijnaoe.2015.09.001.

Mavrakos, S. A., Papazoglou, V. J., Triantafyllou, M. S., & Hatjigeorgiou, J. (1996). Deep-water mooring dynamics. *Marine Structures, 9*(2), 181–209. https://doi.org/10.1016/0951-8339(94)00019-O.

Mavrakos, S. A., & Chatjigeorgiou, J. (1997). Dynamic behavior of deep-water mooring lines with submerged buoys. *Computers and Structures, 64*(1–4), 819–835. https://doi.org/10.1016/S0045-7949(96)00169-1.

Odijie, A. C., Wang, F., & Ye, J. (2017). A review of floating semi-submersible hull systems: Column stabilized unit. *Ocean Engineering, 144*, 191–202. https://doi.org/10.1016/j.oceaneng.2017.08.020.

Ormberg, H., & Larsen, K. (1998). Coupled analysis of floater motion and mooring dynamics for a turret-moored ship. *Applied Ocean Research, 20*(1–2), 55–67. https://doi.org/10.1016/S0141-1187(98)00012-1.

Qiao, D., & Ou, J. (2013). Global responses analysis of a Semi-submersible platform with different mooring models in the South China Sea. *Ships and Offshore Structures, 8*(5), 441–456. https://doi.org/10.1080/17445302.2012.718971.

Stansberg, C. T. (2008). Current effects on a moored floating platform in a sea state. In *ASME 2008 27th International Conference on Offshore Mechanics and Arctic Engineering*. American Society of Mechanical Engineers Digital Collection. 433–444, https://doi.org/10.1115/OMAE2008-57621

Sunil, D. K., & Mukhopadhyay, M. (1995). Free vibration of semi-submersibles: A parametric study. *Ocean Engineering, 22*(5), 489–502. https://doi.org/10.1016/0029-8018(94)00012-V.

Umar, A., Ahmad, S., & Datta, T. K. (2004). Stability analysis of a moored vessel. *Journal of Offshore Mechanics and Arctic Engineering, 126*(2), 164–174. https://doi.org/10.1115/1.1710873.

Wang, K., Er, G. K., & Iu, V. P. (2018). Nonlinear vibrations of offshore floating structures moored by cables. *Ocean Engineering, 156*, 479–488. https://doi.org/10.1016/j.oceaneng.2018.03.023.

Xu, S., Ji, C. Y., & Soares, C. G. (2018). Experimental and numerical investigation a semi-submersible moored by hybrid mooring systems. *Ocean Engineering, 163*, 641–678. https://doi.org/10.1016/j.oceaneng.2018.05.006.

Xue, X., Chen, N. Z., Wu, Y., Xiong, Y., & Guo, Y. (2018). Mooring system fatigue analysis for a Semi-submersible. *Ocean Engineering, 156*, 550–563. https://doi.org/10.1016/j.oceaneng.2018.03.022.

Yan, J., Qiao, D., & Ou, J. (2018). Optimal design and hydrodynamic response analysis of deep-water mooring systems with submerged buoys. *Ships and Offshore Structures, 13*(5), 476–487. https://doi.org/10.1080/17445302.2018.1426282.